



Estimation of the appropriate sampling interval for rock joints roughness using laser scanning

Yunfeng Ge¹ · Zishan Lin¹ · Huiming Tang^{1,2} · Binbin Zhao³

Received: 12 June 2020 / Accepted: 24 February 2021 / Published online: 8 March 2021
© Springer-Verlag GmbH Germany, part of Springer Nature 2021

Abstract

The rock joint roughness greatly affects the mechanical behaviors and permeability characteristics of rock mass. To accurately and effectively estimate the roughness of rock joints, an appropriate sampling interval is required to be specified during the point cloud collection using laser scanning systems and the roughness coefficient calculation. Firstly, seventeen point clouds of rock joints with sampling size ranging from 60×60 to 2000×2000 mm was collected using a terrestrial laser scanner in the field to investigate the effect of sampling size on the selection of the appropriate sampling interval. Then, a portable laser scanner was employed to acquire the dense point clouds of thirteen small-scale rock joint specimens, which have various roughness levels, to assess the influence of roughness level on the appropriate sampling interval. Furthermore, fitting analyses were performed to establish relationships between the appropriate sampling interval vs. sampling size and the appropriate sampling interval vs. roughness level, respectively. The results show that the curves of sampling interval vs. roughness coefficient followed a power distribution, and the inflection point with the maximum curvature could be regarded as the appropriate sampling interval; the appropriate sampling interval increased with the sampling size, while a negative correlation between the appropriate sampling interval and roughness level was observed. To facilitate the application of findings into practical engineering, a simplified workflow was provided to determine the appropriate sampling interval: 0.015×sampling size and 0.03×sampling size were recommended to be considered as appropriate sampling intervals for the rock joints with high-level and low-level roughness, respectively.

Keywords Rock joint roughness · Appropriate sampling interval · Sampling size effect · Roughness level effect · Laser scanning

Introduction

Rock joint roughness is one of the most important inputs for rock mass stability analysis in engineering design due to its significant impact on the shear strength and hydraulic properties of rock mass (Kulatilake et al. 1995; Belem et al. 2007; Liu et al. 2016; Tang et al. 2019; Jiang et al. 2020). Several indexes have been developed to represent the roughness of

rock joint, such as joint roughness coefficient (JRC) (Barton 1973; Barton and Choubey 1977), fractal dimension (Xie et al. 1997; Kulatilake et al. 2006; Stigsson and Ivars 2019), $\theta_{\max}^*/(C+I)$ (Grasselli and Egger 2003), and brightness area percentage (BAP) (Ge et al. 2014). Among them, as the first parameter proposed for rock joint roughness, JRC is more popular in the rock mechanics community because it is relatively straightforward (ISRM 1978). JRC can be determined through visual comparison with ten standard profiles; however, it is highly dependent on people's subjective judgment, causing roughness estimation errors. To solve this issue, several quantitative approaches were developed to build quantitative relationships between JRC and statistical parameters, including root mean square (Z_2) (Tse and Cruden 1979), standard deviation of inclination angle (SD_i) (Kusumi et al. 1997), fractal dimension (Lee et al. 1990; Lee et al. 1997), and power spectral density (Ünlüsoy and Sützen 2020). Recently, artificial intelligence (AI) algorithms have been employed to

✉ Huiming Tang
tanghm@cug.edu.cn

¹ Faculty of Engineering, China University of Geosciences, Wuhan, Hubei, China

² Three Gorges Research Center for Geohazards, China University of Geosciences, Ministry of Education, Wuhan, Hubei, China

³ Research Institute of Transmission and Transformation Projects, China Electric Power Research Institute Co., Ltd, State Grid Corporation of China, Beijing, China

predict the JRC through data training (Wang et al. 2017; Wang et al. 2020).

Several techniques were available to collect the morphology data of the rock joint surface (e.g., 2D profiles or 3D point clouds), which was treated as input parameters to determine the JRC for above-mentioned quantitative approaches. To date, data collection was mainly subdivided into two categories: contact method and non-contact method (Feng et al. 2003). A contact method was often characterized by time-consuming and low precision, especially for large-scale measurement. Therefore, there was an increasing interest in the non-contact method which mainly involves laser scanning and photogrammetry (Maerz et al. 1990; Jiang et al. 2006; Bae et al. 2011; Kim et al. 2013; Mah et al. 2013; Ge et al. 2017). Among these two non-contact techniques, laser scanning was considered as a powerful tool to collect dense point clouds of rock joint surfaces in a short time (Tang et al. 2012; Kumar and Verma 2020). In this study, two kinds of laser scanner were employed to map the rock joints: a terrestrial laser scanner for a larger scale bedding plane in the field and a portable one for small-scale rock joint specimens in the laboratory.

Numerous attempts have been made to investigate the influence of sampling scale, anisotropy, and non-stationary features on the roughness estimation of rock joint (Fardin et al. 2001; Tatone and Grasselli 2013; Kumar and Verma 2016; Ge et al. 2020). Similarly, the sampling interval (also termed sampling spacing) also has a significant impact on the data collection and roughness assessment, which was defined as the horizontal distance between two adjacent points in 2D profiles or 3D point clouds of rock joints and was directly related to the measurement resolution (Yu and Vayssade 1991). On one hand, natural rock joints always consist of two kinds of asperities: primary and secondary asperity (waviness and unevenness, non-stationary and stationary), which represents the macroscopic undulation and microscopic irregularity of the rock joint surface, respectively (Patton 1966; ISRM 1978; Yang et al. 2010). An appropriate sampling interval is needed to be selected to capture these different-scale morphological characteristics (Liu et al. 2017). On the other hand, during a laser scanning, high-resolution point clouds of a rock joint were generated under a small sampling interval, allowing acquisition of more details on the rock joint surface. However, measurement with extra high resolution tended to produce a large number of redundancy, as a result, causing overestimation on roughness and low computational efficiency. Accordingly, a high level of hardware and software capacity was required for data processing. On the other hand, if a too large sampling interval was assigned for laser scanning measurement, lots of geometrical information on the rock joint surface would be ignored, leading to an underestimation on the roughness, even for a very rough rock joint (Reeves 1985; Tatone and Grasselli 2010).

Up to now, some researches have focused on the effect of sampling interval on the estimation of rock joint roughness (Hong et al. 2008; Ge et al. 2015; Sun et al. 2019). A negative correlation between the rock joint roughness and sampling interval was observed in their findings (Ge et al. 2013; Yong et al. 2018; Han et al. 2020). Unfortunately, there was still a lack of effective methods to determine the appropriate sampling interval both considering the effect of sampling size and roughness level.

This paper aims to provide a method to determine the appropriate laser scanning sampling interval for calculating the JRC based on sampling size and roughness level of rock joint. Using a terrestrial and a portable laser scanner, point clouds collection was conducted both in the field and laboratory to assess the effect of sampling size and roughness level on the selection of appropriate sampling size, respectively. Furthermore, a method was proposed to determine the appropriate sampling interval from the curves of the roughness coefficient vs. sampling interval based on a power function. Eventually, a simplified workflow was provided to promptly determine the appropriate sampling interval for engineering practice.

Point clouds collection of rock joints

Point clouds collection of large-scale rock discontinuities

Point clouds of a large-scale rock discontinuity were collected in situ to investigate the effects of sampling size on the selection of the appropriate sampling interval. This rock discontinuity was exposed at an easy-access outcrop in Jiweishan landslide region in Wulong County, Chongqing City, southwest of China, which belonged to a bedding plane with an orientation of $350^{\circ}\angle 30^{\circ}$. The major rock lithology in the study area is the grayish-black medium-thick limestone from Feixianguan formation in Triassic (T_1f). A terrestrial laser scanner—Optech ILRIS-3₆D—was employed to acquire the point cloud of the discontinuity surface. The laser scanner had to be installed near the middle of the road due to the limited space. The average distance between the scanning object and the laser scanner is 11.31 m, and the sampling interval was specified as 1 mm. In this manner, the region of interest (ROI) with a dimension of 2300×2300 mm was digitized into about 5,544,113 points, and the whole scanning period lasted approximately 15 min (Fig. 1). Seventeen concentric square-shaped sampling windows were extracted from the point cloud, ranging from 60×60 to 2000×2000 mm (Fig. 2).

Fig. 1 In situ point clouds acquisition: **a** configuration of a terrestrial laser scanner; **b** ROI locates in the red quadrilateral



(a)



(b)

For each sampling window, the downsampling was performed to produce 100 new point clouds based on the original point cloud, resulting in main geometric features that were preserved but with different sampling intervals. The downsampling refers to a process of resampling point clouds with a low resolution from the original point cloud. It is time-consuming and impossible to perform 1900 scans to acquire point clouds with 100 different sampling intervals for each sampling windows using a terrestrial laser scanner in the field survey, due to the heavy workload and limited battery capacity. To reduce the testing time, the downsampling algorithm was employed to generate different resolution point clouds based on the original point cloud of the rock joint (sampling interval = 1 mm). The maximum sampling interval was equal to the half of the side of the sampling window, while the

minimum one was set to the original sampling interval (1 mm).

Point clouds collection of laboratory-scale rock joints

To assess the effects of roughness degree of rock joint on the selection of appropriate sampling intervals, thirteen approximately square rock joint specimens with different roughness levels were chosen for laser scanning in the laboratory. Specimens had similar length of the side, varying from 60.35 to 71.00 mm. The rock type of specimens is quartz sandstone which belongs to Upper Jurassic Suining Formation (J_3s) exposed in the Majiagou landslide region in Zigui County, Yichang City, Hubei Province, Central China. A portable laser scanner, OKIO-FreeScan X5, was utilized to

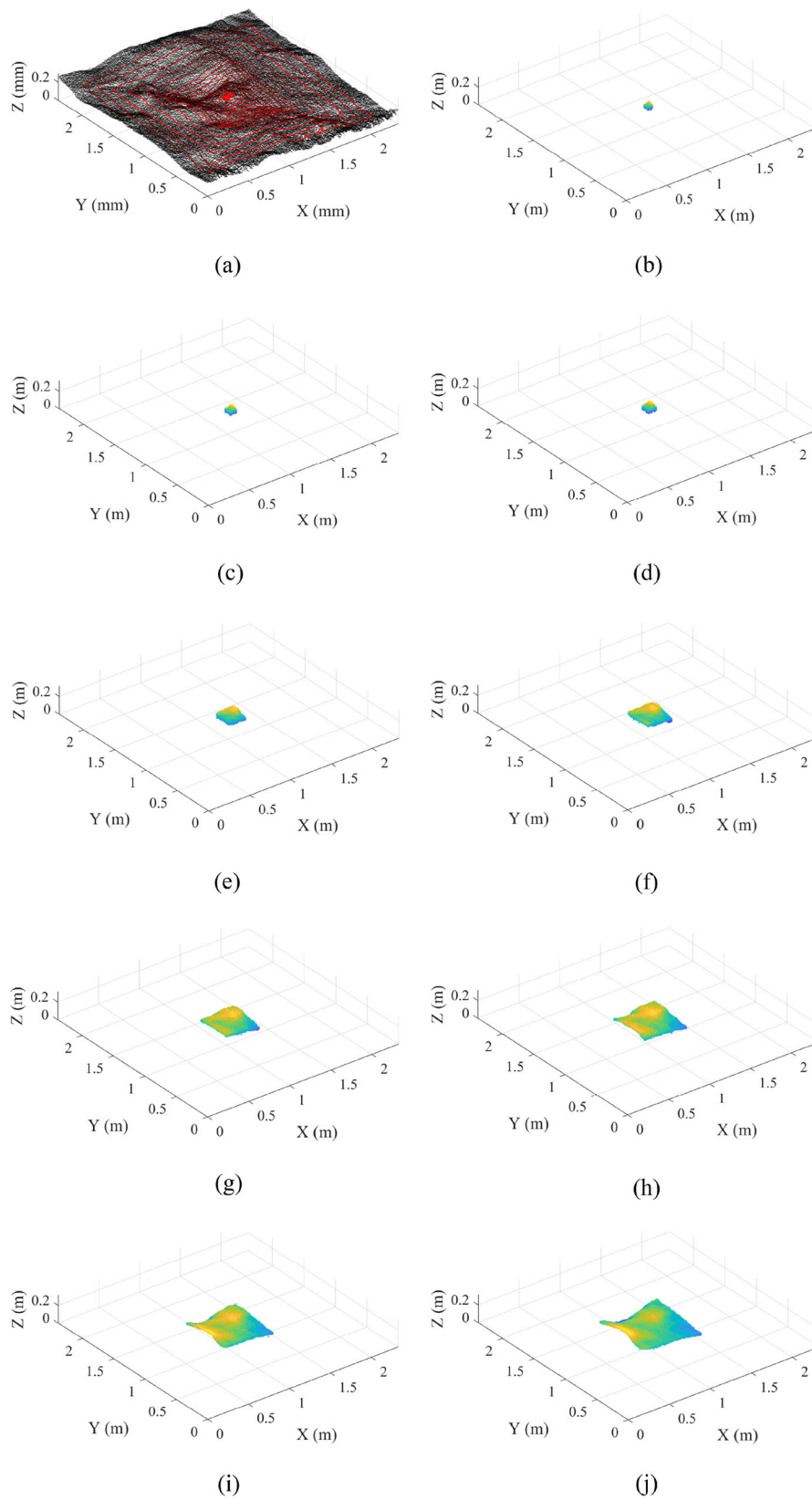


Fig. 2 Seventeen sampling windows with different scales: **a** locations of various sampling windows in original point clouds, **b** 60×60 mm, **c** 80×80 mm, **d** 100×100 mm, **e** 200×200 mm, **f** 300×300 mm, **g**

h 400×400 mm, **h** 500×500 mm, **i** 600×600 mm, **j** 700×700 mm, **k** 800×800 mm, **l** 900×900 mm, **m** 1000×1000 mm, **n** 1200×1200 mm, **o** 1400×1400 mm, **p** 1600×1600 mm, **q** 1800×1800 mm, **r** 2000×2000 mm

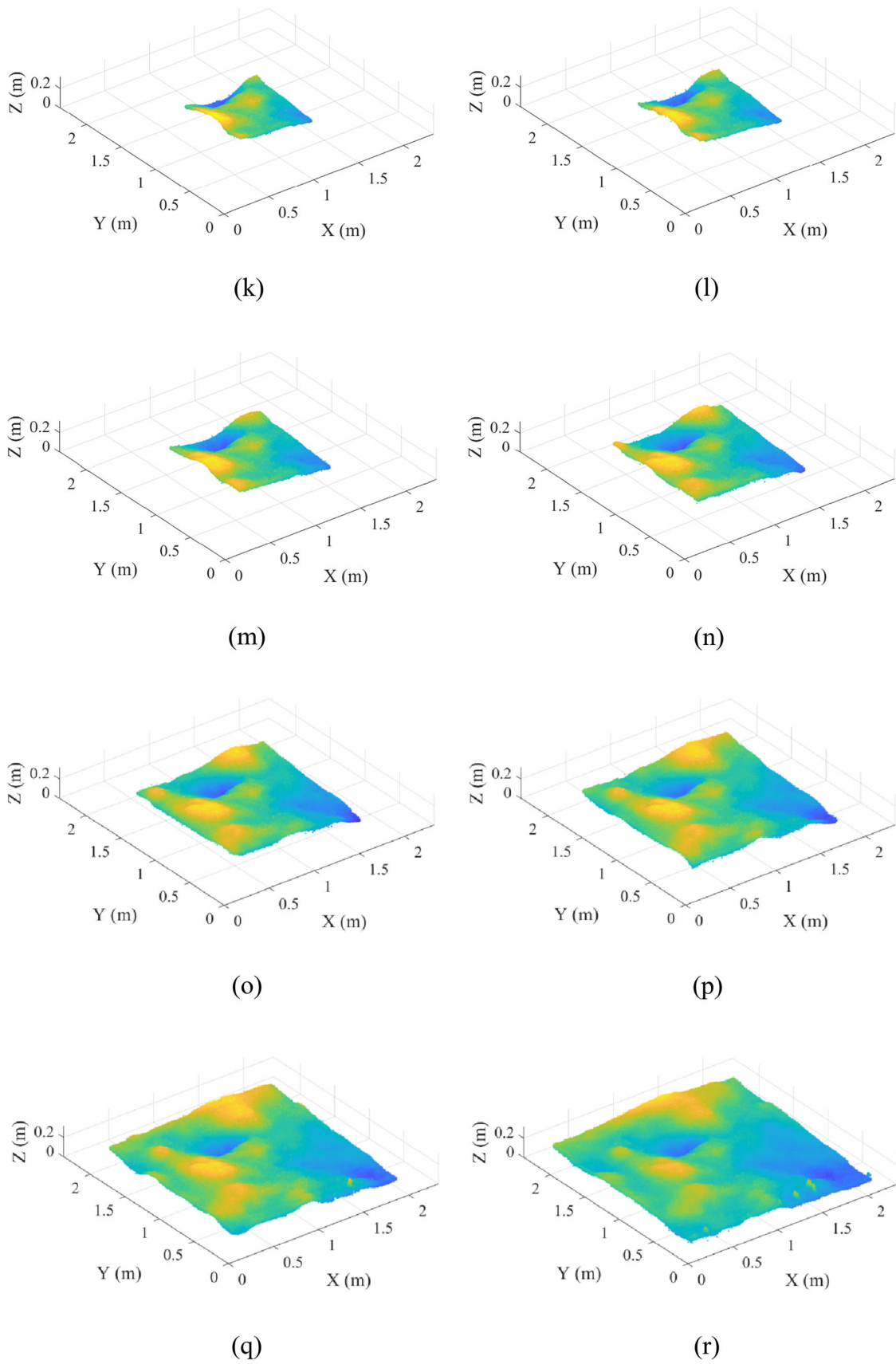
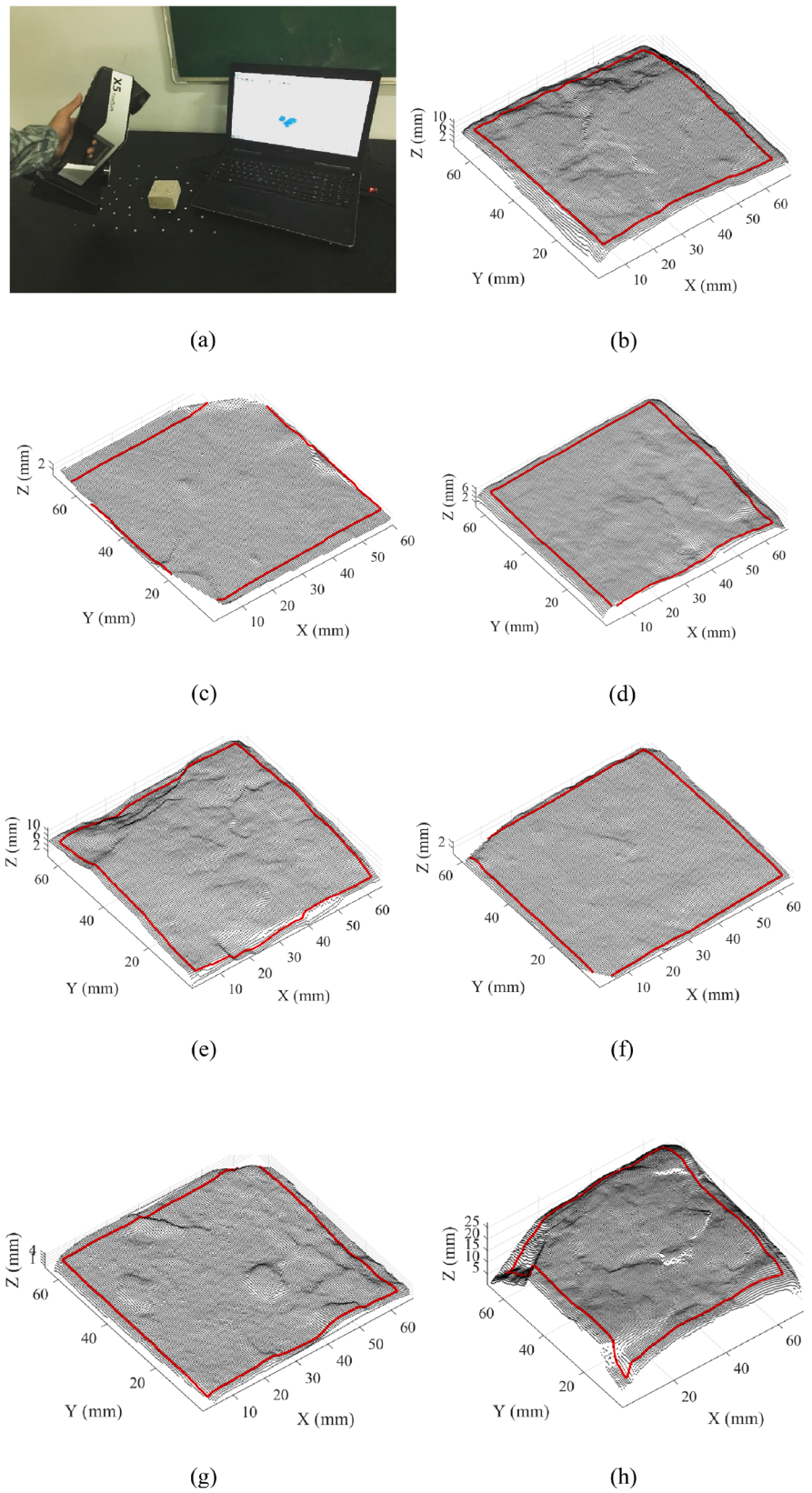


Fig. 2 (continued)

Fig. 3 Original point clouds and regions of interest (red frames) of 13 rock joint specimens in laboratory (to display clearly, the point clouds were illustrated based on a sampling interval of 0.5 m): **a** configuration of portable laser scanner, **b** JS-1, **c** JS-2, **d** JS-3, **e** JS-4, **f** JS-5, **g** JS-6, **h** JS-7, **i** JS-8, **j** JS-9, **k** JS-10, **l** JS-11, **m** JS-12, **n** JS-13



capture the point clouds of these specimens. Several target points with a 3-mm diameter were placed around joint

specimens, allowing to accurately merge together multiple scans into a composite point clouds through aligning the

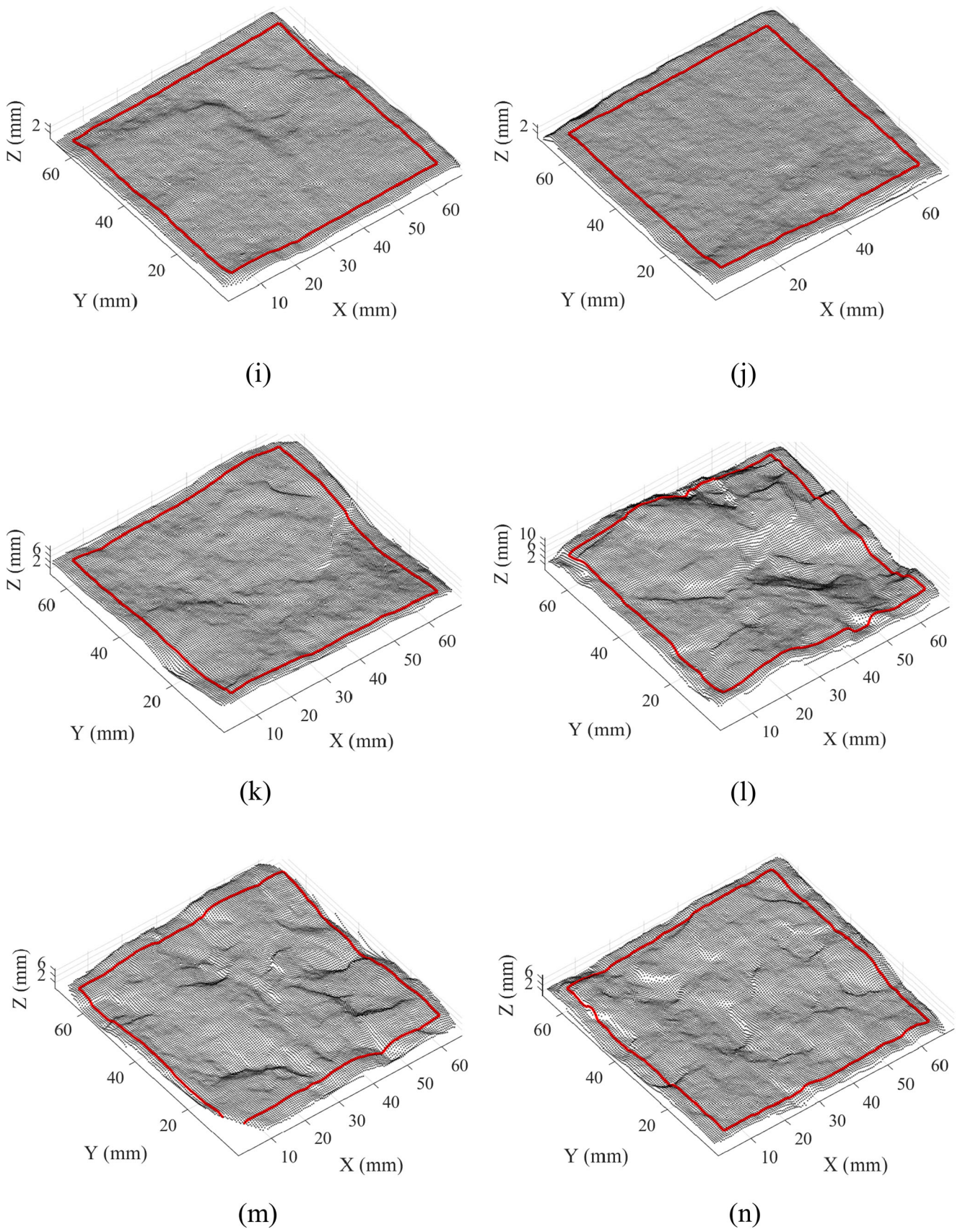
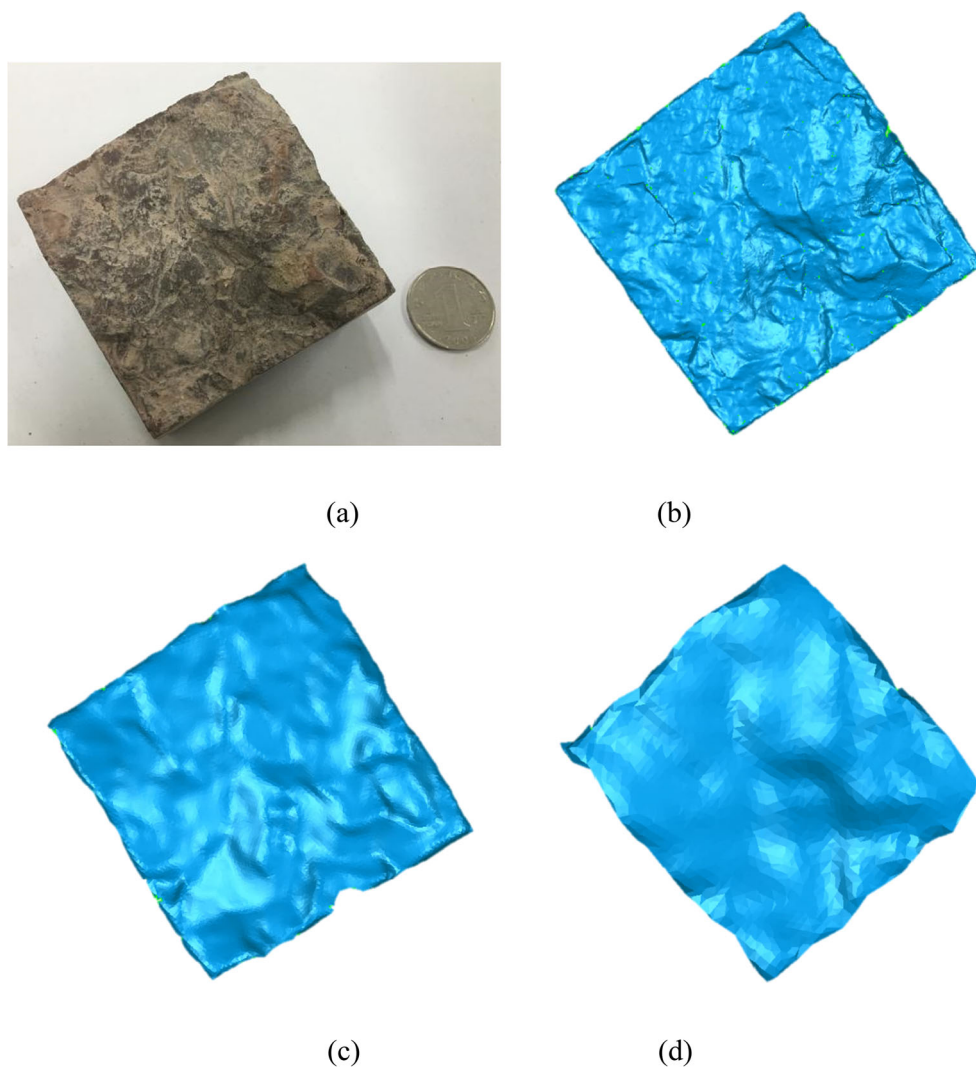


Fig. 3 (continued)

Fig. 4 Effect of sampling interval on the 3D reconstruction of a rock joint specimen: **a** top view of JS-5 joint specimen, **b** sampling interval = 1 mm, **c** sampling interval = 2 mm, **d** sampling interval = 5 mm



common target points to each scan. Some parameters are required to be input before scanning, and the light-emitting diode (LED) lightness level and optical intensity were appointed as 550 and 600, respectively, according to object texture, object color, and surrounding light conditions. To obtain dense point clouds of rock joint specimens, the sampling interval was set as 0.05 mm—the highest resolution the scanner can achieve. More importantly, to eliminate the influence of sampling size on the analysis, sampling windows with a fixed size of 60×60 mm were extracted from the original point cloud for each rock joint specimen (areas within the red frame in Fig. 3). In this manner, near two million points were gained for each specimen, ensuring enough resolution for performing the estimation of the effect of roughness level on the appropriate sampling interval.

Similar to the field survey, the downsampling algorithm was applied again to generate a series of point clouds for each specimen with 200 different sampling intervals ranging from 0.05 to 10.00 mm with a 0.05 mm step size. Figure 4 shows

the 3D models of JS-5 that were reconstructed based on point clouds with intervals of 1 mm, 2 mm, and 5 mm. The sampling interval has a significant impact on the rock joint roughness. More details tended to be missed with the increase of interval, causing a smoother joint surface, while model provides more microstructural characteristics of the joint specimen with a smaller interval.

Methods for estimation of rock joint roughness and appropriate sampling interval

Although many approaches have been proposed for characterizing the roughness of rock joint, JRC is the most widely used parameter and has been adopted as a standard method, because of its easy operation and good reliability (Alameda-Hernández et al. 2014). Therefore, JRC was selected as the index to describe the roughness of rock joints in this study. For each joint specimen with a certain

Fig. 5 Extraction of 2D profiles from rock joint point clouds with different sampling intervals (just taking 4 sampling intervals for demonstration): **a** sampling interval = 0.5 mm, **b** sampling interval = 0.7 mm, **c** sampling interval = 1.0 mm, **d** sampling interval = 5.0 mm

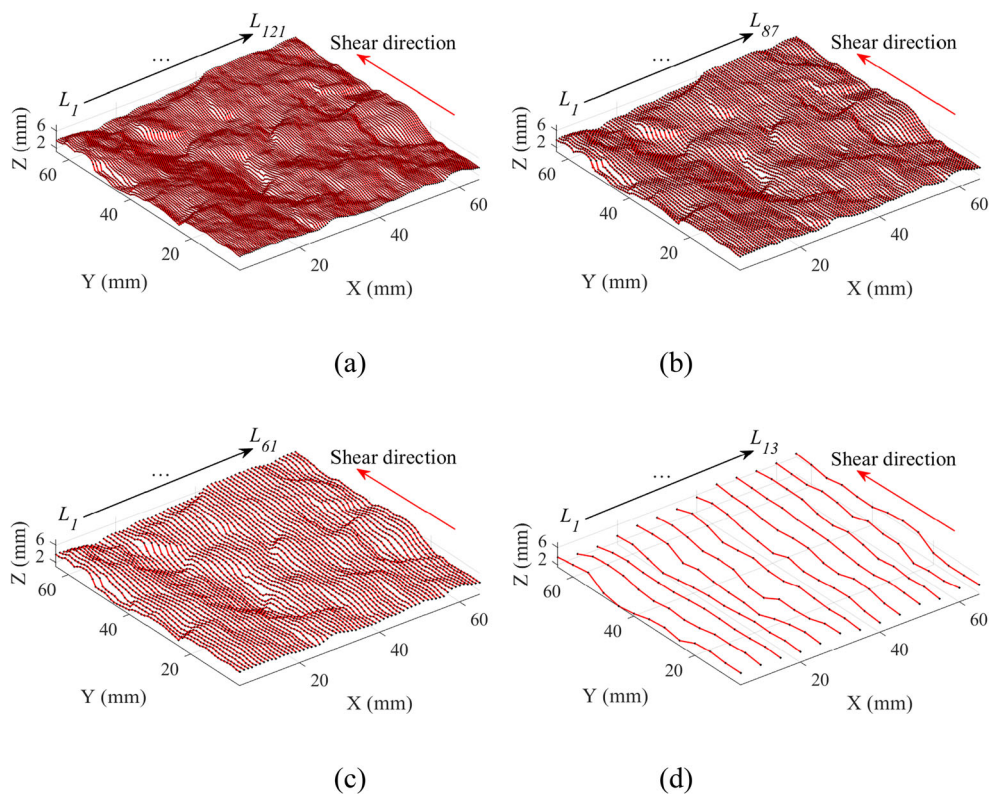
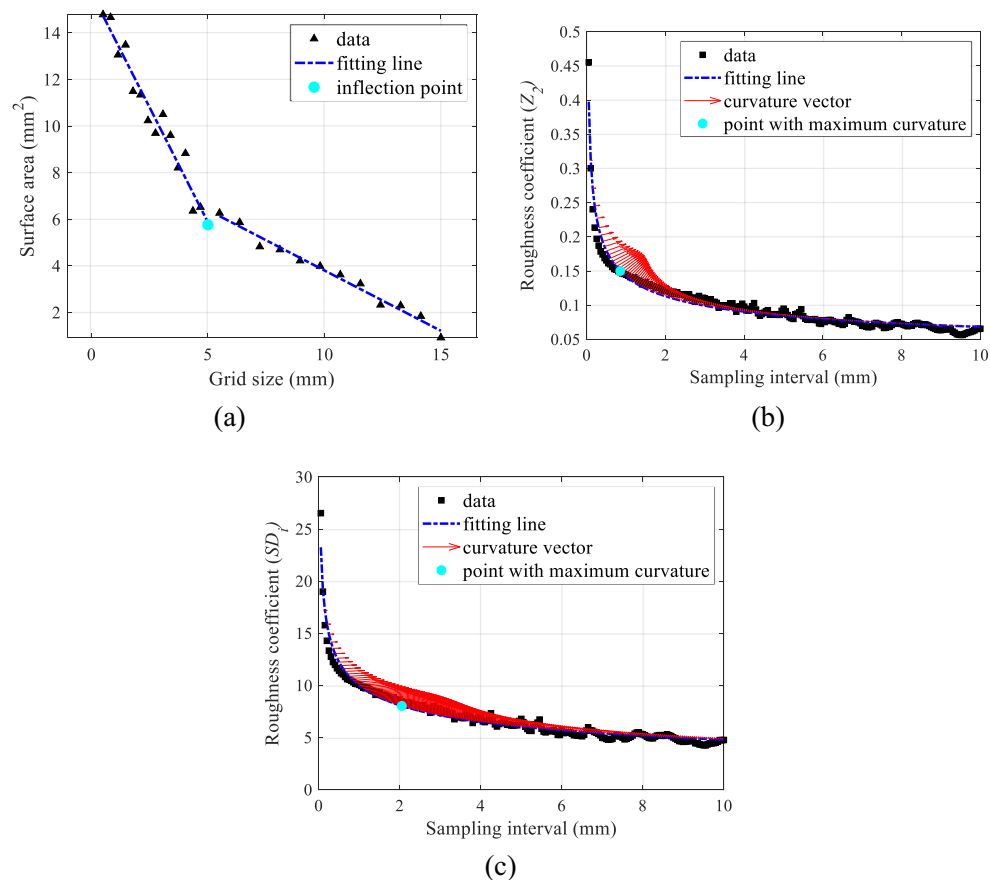


Fig. 6 Schematic diagram of searching the appropriate sampling interval using: **a** dual-linear function, **b** power function for Z_2 , and **c** power function for SD_i



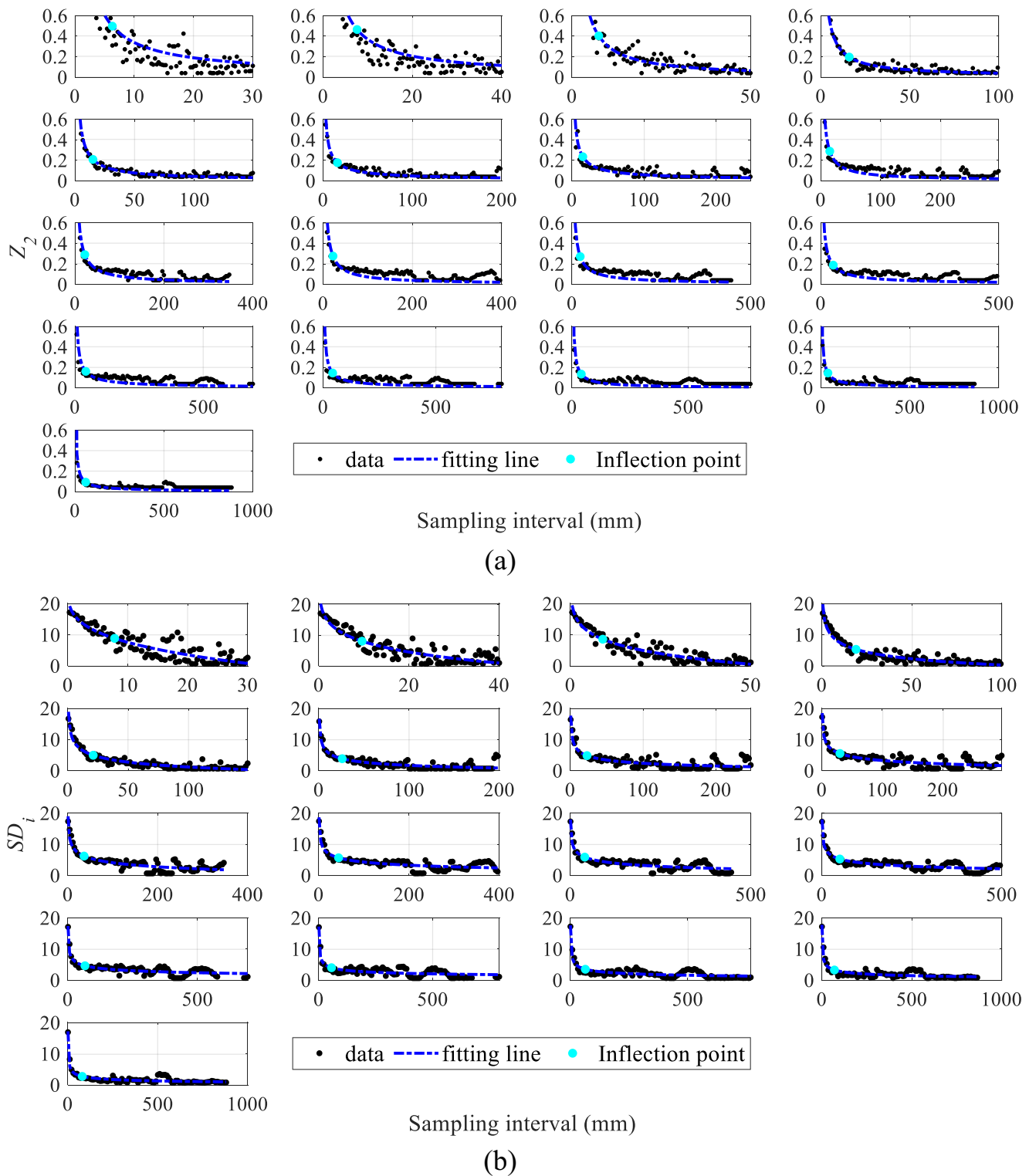


Fig. 7 Curves of sampling interval vs. roughness coefficient for seventeen larger-scale rock joint specimens: **a** Z_2 and **b** SD_i

sampling interval, a series of profiles along the shear direction were extracted from the point cloud with a step size equaling to the sampling interval, so that there are a sufficient number of profiles to capture morphology features of rock joints in 3D level (Fig. 5). For example, if

the sampling interval of a point cloud is 0.05 mm and the sampling size is 60×60 mm, 1201 profiles ($60/0.05 + 1 = 1201$) will be generated in total.

JRC^{2D} for each 2D profile was computed based on two widely used parameters of Z_2 and SD_i , respectively, which

Table 1 Fitting parameters and appropriate sampling intervals for 17 large-scale rock discontinuities

No	Size (mm)	<i>a</i>		<i>b</i>		<i>k</i> _{max}		Appropriate sampling interval (mm)	
		<i>Z</i> ₂	<i>SD</i> _{<i>i</i>}	<i>Z</i> ₂	<i>SD</i> _{<i>i</i>}	<i>Z</i> ₂	<i>SD</i> _{<i>i</i>}	<i>Z</i> ₂	<i>SD</i> _{<i>i</i>}
1	60	5.7995	80.1435	-0.8353	-0.4029	0.0462	0.0368	6.3	7.8
2	80	6.4132	86.6139	-0.8415	-0.4308	0.0305	0.0391	7.6	9.6
3	100	7.1388	90.9351	-0.9707	-0.455	0.0335	0.036	7.5	9
4	200	5.5647	84.5369	-0.8744	-0.4641	0.0032	0.0281	16	19
5	300	4.9312	78.6156	-0.8283	-0.4527	0.0035	0.023	15	21
6	400	3.1721	67.1661	-0.7097	-0.4241	0.0021	0.0135	16	26
7	500	4.2598	72.0398	-0.7303	-0.3843	0.0033	0.0181	15	23
8	600	7.7954	78.7281	-0.878	-0.3441	0.0053	0.0112	15	30
9	700	9.8457	84.1002	-0.8427	-0.3187	0.0023	0.008	22	36
10	800	10.4077	80.3206	-0.8765	-0.2933	0.0024	0.005	22	44
11	900	9.0939	78.7849	-0.8267	-0.2949	0.0019	0.006	23	40
12	1000	8.4283	77.2012	-0.8105	-0.2938	0.0006	0.0036	35	50
13	1200	7.2552	73.405	-0.7701	-0.2834	0.0003	0.0018	42	66
14	1400	6.5745	69.5996	-0.7715	-0.3087	0.0003	0.0025	42	56
15	1600	7.9831	70.3649	-0.8542	-0.3432	0.0003	0.0019	40	64
16	1800	7.8178	70.4345	-0.8288	-0.3564	0.0003	0.0015	40	70
17	2000	6.0317	67.1671	-0.7945	-0.3703	0.0001	0.001	60	80

were capable of characterizing the roughness of rock joints accurately and quickly (Eqs. 1, 2, 3, 4, and 5), due to the strong correlation with JRC, straightforward calculation, and high computational efficiency (Tse and Cruden 1979; Kusumi et al. 1997; Yang et al. 2001; Jang et al. 2014).

$$Z_2 = \sqrt{\frac{1}{L} \sum_{j=1}^{N-1} \frac{(z_{j+1} - z_j)^2}{y_{j+1} - y_j}} \tag{1}$$

$$JRC^{2D} = 32.2 + 32.47 \cdot \log_{10} Z_2 \tag{2}$$

$$SD_i = \tan^{-1} \sqrt{\frac{1}{L} \sum_{j=1}^{N-1} \left(\frac{z_{j+1} - z_j}{y_{j+1} - y_j} - \tan i_{ave} \right)^2 \cdot (y_{j+1} - y_j)} \tag{3}$$

$$i_{ave} = \tan^{-1} \left(\frac{1}{L} \sum_{j=1}^{N-1} |z_{j+1} - z_j| \right) \tag{4}$$

$$JRC^{2D} = 1.14 \cdot SD_i - 3.88 \tag{5}$$

where z_{j+1} and z_j are the Z coordinates of $(j+1)$ th and j th points in the given profile; y_{j+1} and y_j are the Y coordinates of $(j+1)$ th and j th points; N is the total points number of the profile, L is the profile length; and i_{ave} is the average inclination angle.

Ultimately, the JRC of a rock joint was determined by averaging JRC^{2D} for all profiles (Eq. 6).

$$JRC = \frac{1}{M} \sum_{k=1}^M JRC_k^{2D} \tag{6}$$

where M is the total profile number of the given rock joint specimen and k is the k th profile. Note that roughness calculations were carried out after removing the non-stationary features for the laboratory-scale rock joints, which represents large-scale undulation of the rock joint surface and can be eliminated through coordinate transformation. For more details about the removal of non-stationary features, please refer to Ge et al. (2020).

The inflection point method was referred to determine the appropriate sampling interval in this study, which was originally proposed to separate the large-scale undulation and small-scale unevenness based on the plots of grid size vs. surface area (Fig. 6a) (Sun et al. 2019; Li et al. 2018). Figure 6 b and c illustrate typical plots of the roughness coefficient (i.e., Z_2 and SD_i) vs. sampling interval. The roughness coefficients dropped sharply when small sampling intervals were specified; then roughness coefficients experienced a gradual decrease with the increase of sampling interval as the sampling interval continued beyond a certain point (appropriate sampling interval); eventually, the roughness coefficients fluctuated along with a constant. That is, the roughness coefficients were more sensitive to small sampling interval than the large one. When the sampling interval was specified less than the appropriate sampling interval, although more

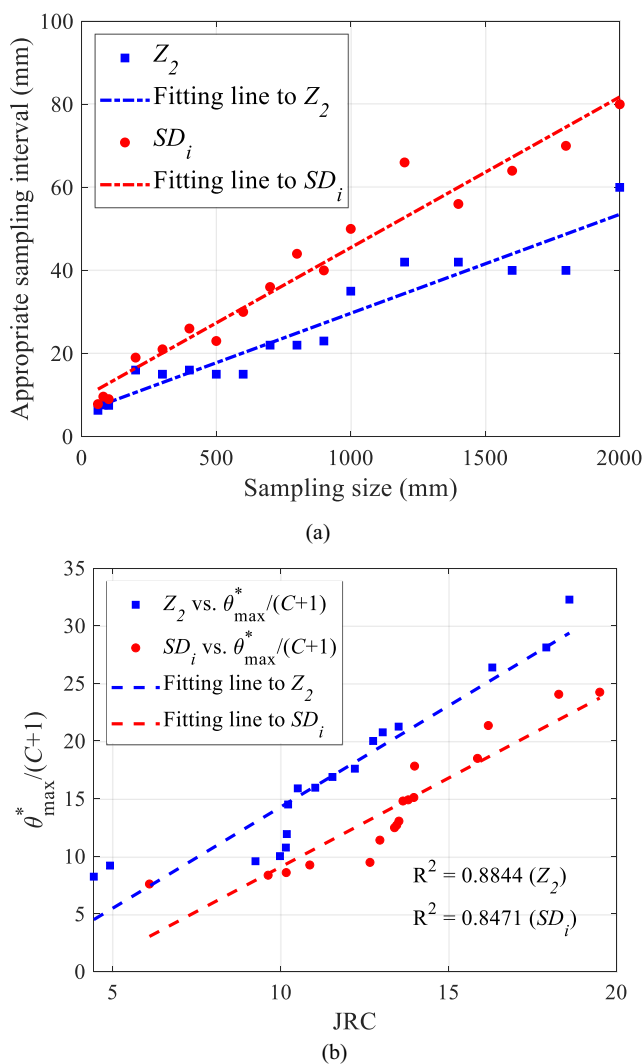


Fig. 8 Roughness estimation for large-scale rock discontinuities: **a** relationship between sampling size and appropriate sampling interval and **b** comparison of roughness estimation between Grasselli's method and our methods using Z_2 and SD_i

details on the morphology of rock joint surfaces could be captured, the roughness was overestimated, making the evaluations unreliable. Nevertheless, if the sampling interval was set larger than appropriate sampling interval, the change in roughness coefficients tended to be stable; however, many surface details of rock joint would be ignored, resulting in underestimation of rock joint roughness. Therefore, errors caused by the effect of sampling interval can be eliminated when collecting the point clouds with an appropriate sampling interval.

Rock joint roughness always presents a strong nonlinear characteristic so that the linear fitting (Fig. 6a) is no longer suitable for this issue. Additionally, previous work did not provide a method to exactly locate the inflection point. In this study, the above-mentioned approach was modified to detect the inflection point from the curve of the sampling interval vs.

roughness coefficient as the appropriate sampling interval. To describe the nonlinear characteristics of the rock joint roughness, a power function was used to create the fit to the data instead of the dual-linear function (Eq. 7).

$$RC = a \times SI^b \quad (7)$$

where RC is the roughness coefficient, such as Z_2 and SD_i ; SI denotes the sampling interval; and a and b are the fitting parameters that need to be determined. The length of the curvature vector (k) of each point in the power fitting line can be defined as,

$$k = \frac{|RC'|}{(1 + RC'^2)^{\frac{3}{2}}} = \frac{a \times b \times (b-1)SI^{b-2}}{[1 + (a \times b \times SI^{b-1})^2]^{\frac{3}{2}}} \quad (8)$$

Then, the point with the maximum length of the curvature (k_{\max}) was considered as the appropriated sampling interval in the curve (cyan dots in Fig. 6 b and c). To facilitate the utility of Eqs. (7) and (8) to find the appropriate sampling interval in a simple way, the main steps were given: ① obtain the plots of roughness coefficients (Z_2 and SD_i) vs. sampling interval; ② determine the fitting parameters a and b through fitting power function curves (Eq. 7) to the plots of roughness coefficient (Z_2 and SD_i) vs. sampling interval in step (1); ③ calculate the length of the curvature vector k for each sampling interval, which is a function of a , b , and sampling interval (Eq. 8); and ④ find the maximum k values (k_{\max}), and the sampling interval with the k_{\max} is regarded as the appropriate sampling interval.

Influence of rock joint size on the appropriate sampling interval

For the large-scale rock discontinuity in situ situations, roughness coefficients (Z_2 and SD_i) of 17 rock joint specimens with different sizes were calculated under different sampling intervals. Figure 7 shows that all roughness coefficients (Z_2 and SD_i) decreased with the increase of sampling interval. For a small sampling interval, a sharp decrease of roughness coefficients was observed, while the roughness coefficients experienced a gradual reduction when the sampling interval became large.

Table 1 summarizes the fitting parameters a and b for 17 different-scale rock discontinuities, which were determined through fitting power function curves (Eq. 7) to the plots of Z_2 vs. sampling interval and SD_i vs. sampling interval, respectively. The length of the curvature vector k is a function of a , b , and sampling interval SI (Eq. 8). k values for each sampling interval were calculated, and the sampling interval with a maximum k (k_{\max}) was regarded as the appropriate sampling interval (cyan dots in Fig. 7).

Table 2 Summary of roughness estimation for 17 large-scale rock discontinuities using three methods and appropriate sampling intervals

No	Size (mm)	JRC		C		θ_{max}^*		$\theta_{max}^*/(C + 1)$	
		Z_2	SD_i	Z_2	SD_i	Z_2	SD_i	Z_2	SD_i
1	60	18.60	19.50	1.065	1.4526	66.626	59.4375	32.2637	24.2341
2	80	17.91	16.18	1.0388	1.8963	57.3175	61.8071	28.1139	21.3401
3	100	16.30	18.28	1.581	1.6067	68.0764	62.6952	26.3761	24.0517
4	200	10.22	10.86	3.4121	15.5577	63.9355	153.0463	14.4908	9.2432
5	300	10.51	9.62	1.745	8.6755	43.6186	80.8526	15.8902	8.3564
6	400	4.91	6.09	5.586	10.7520	60.5364	89.2433	9.1917	7.5939
7	500	4.43	10.16	10.5186	7.9950	94.8069	77.2193	8.2308	8.5847
8	600	9.25	13.96	5.6659	1.7160	63.7899	41.0095	9.5695	15.0991
9	700	11.54	15.86	1.6701	2.0971	45.0670	57.2737	16.8785	18.4928
10	800	13.51	13.64	1.2505	4.2743	47.8139	78.0288	21.246	14.7942
11	900	13.04	13.45	1.3472	113.067	48.7110	1448.6465	20.7524	12.7000
12	1000	12.75	13.80	1.4614	16.5379	49.2278	261.2147	20.0000	14.8943
13	1200	12.21	13.39	2.1228	7.8829	54.9492	110.8548	17.5963	12.4796
14	1400	11.03	13.99	2.6477	2.8038	58.1746	67.7829	15.9482	17.8199
15	1600	10.18	13.52	6.2567	1.4665	86.5312	32.1833	11.9243	13.0481
16	1800	10.15	12.95	19.4735	17.0199	220.1747	205.4032	10.7541	11.3987
17	2000	9.98	12.66	11.9588	11.2810	129.7400	116.3048	10.0117	9.4703

It was found that sampling sizes had a significant impact on the appropriate sampling interval (Fig. 8a), and the appropriate sampling interval increased with the increase of sampling size. The relationship between them can be written as,

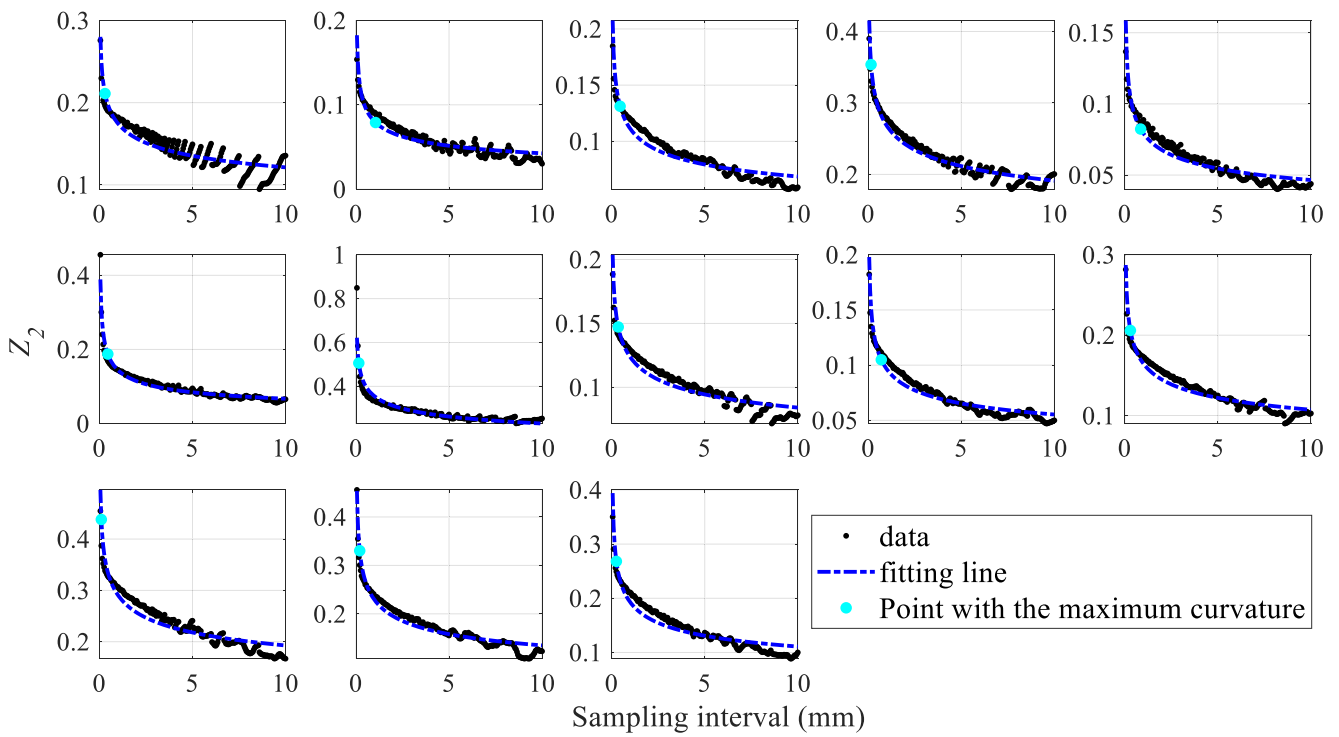
$$\begin{cases} SI_a = 0.0238 \times SS + 5.8479 & 60mm \leq SS \leq 2000mm \quad r^2 = 0.9147 \quad (Z_2) \\ SI_a = 0.0363 \times SS + 9.2085 & 60mm \leq SS \leq 2000mm \quad r^2 = 0.9582 \quad (SD_i) \end{cases} \quad (9)$$

where SI_a indicates the appropriate sampling interval with a unit of mm, SS is the sampling size with a unit of mm, and r^2 is the correlation coefficient.

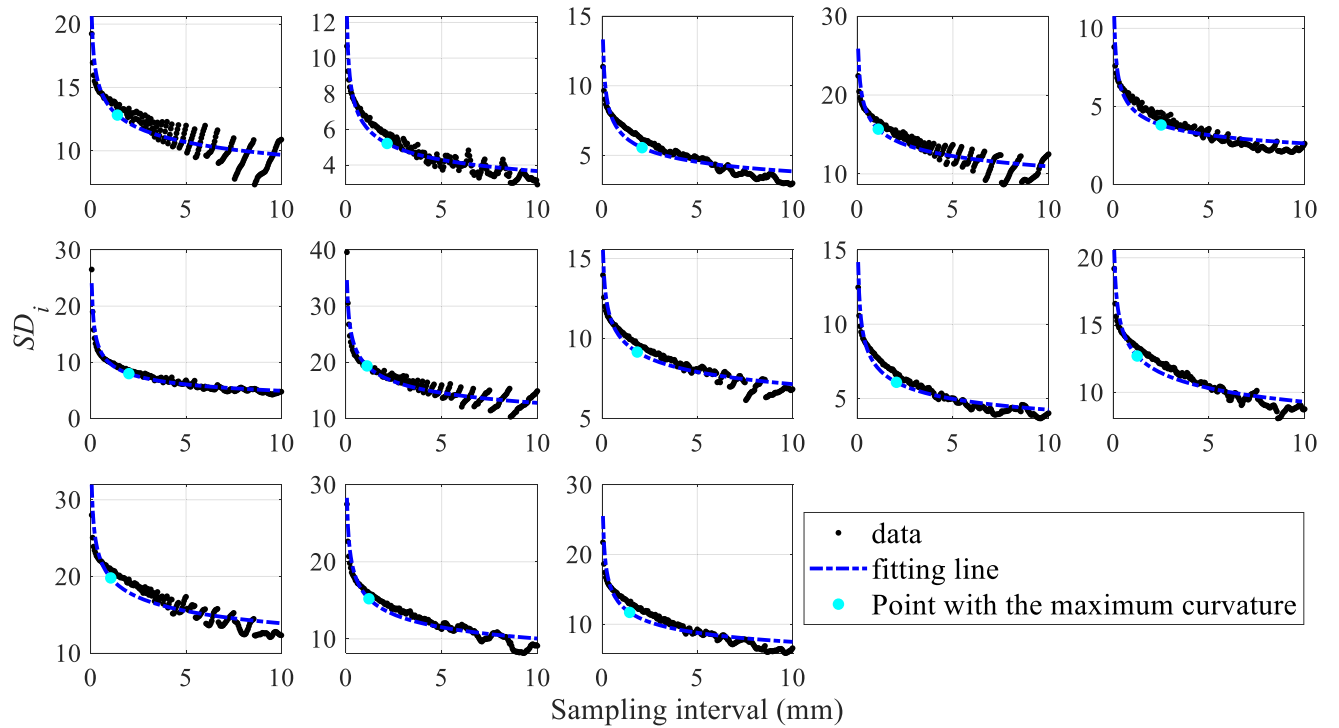
Furthermore, a comparison of rock joint roughness—obtained using Grasselli (2001) and Z_2 and SD_i methods presented in this study, respectively—was performed with the same appropriate sampling interval. Table 2 shows the values of JRC , C , θ_{max}^* , and $\theta_{max}^*/(C + 1)$ for 17 rock discontinuities

Table 3 Fitting parameters and appropriate sampling intervals for 13 small-scale rock joint specimens with different roughness level

No	Size (mm)	a		b		k_{max}		Appropriate sampling interval (mm)	
		Z_2	SD_i	Z_2	SD_i	Z_2	SD_i	Z_2	SD_i
JS-1	60	0.1745	13.4493	-0.158	-0.1428	0.4212	0.2393	0.30	1.40
JS-2	60	0.0801	6.2093	-0.2748	-0.2297	0.0251	0.2124	1.05	2.15
JS-3	60	0.1111	6.6057	-0.2087	-0.2343	0.1626	0.2237	0.45	2.10
JS-4	60	0.2678	15.9181	-0.1465	-0.1622	2.2292	0.1529	0.15	1.10
JS-5	60	0.0793	4.8632	-0.2315	-0.2658	0.0325	0.1633	0.85	2.50
JS-6	60	0.1438	9.8199	-0.3321	-0.2996	0.3981	0.2052	0.45	2.00
JS-7	60	0.3547	19.7051	-0.1873	-0.1883	3.0217	0.0863	0.15	1.10
JS-8	60	0.1236	10.0136	-0.1669	-0.1466	0.2324	0.2385	0.35	1.85
JS-9	60	0.0962	7.1711	-0.2408	-0.2277	0.0638	0.2302	0.70	2.05
JS-10	60	0.1646	13.1317	-0.1859	-0.1499	0.4923	0.2317	0.30	1.25
JS-11	60	0.2906	19.9562	-0.1784	-0.1573	4.5046	0.1066	0.10	1.05
JS-12	60	0.2285	15.7597	-0.229	-0.1954	1.9018	0.1295	0.20	1.20
JS-13	60	0.1924	12.7512	-0.2393	-0.2314	1.1560	0.1669	0.25	1.45



(a)



(b)

Fig. 9 Curves of sampling interval vs. roughness coefficient for thirteen rock joint specimens: **a** Z_2 and **b** SD_i

with different sizes, which were computed based on the appropriate sampling interval mentioned in Table 1. Figure 8 b

illustrates the comparisons of estimation of rock joint roughness based on Z_2 , SD_i and Grasselli's methods, and good

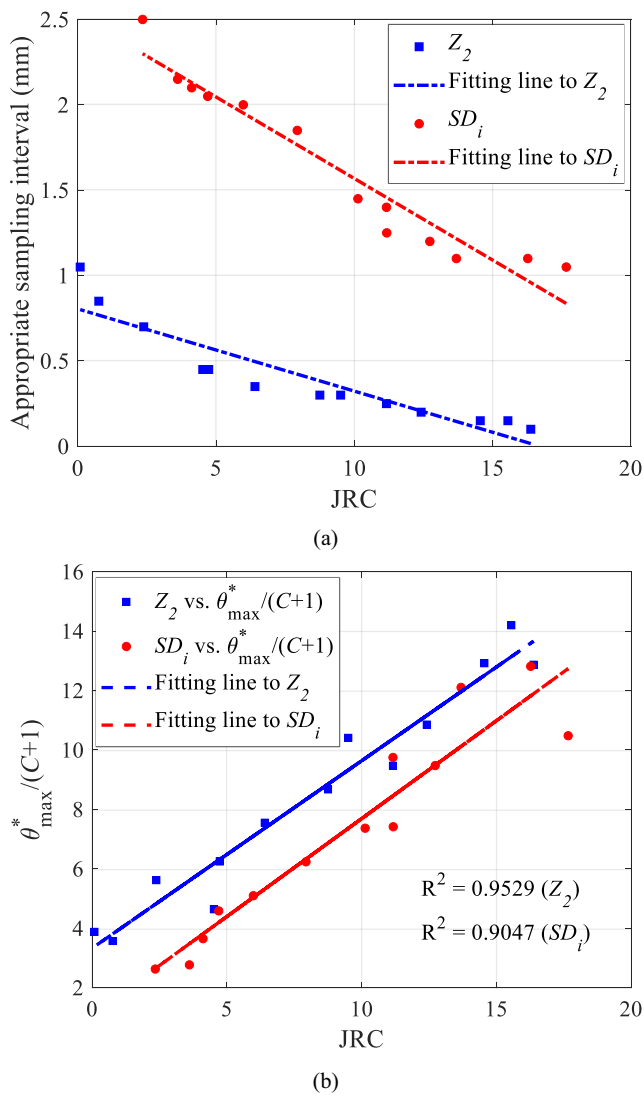


Fig. 10 Roughness estimation for small-scale rock joint specimens: **a** relationship between roughness level and appropriate sampling interval and **b** comparison of roughness estimation between Grasselli’s method and our methods using Z_2 and SD_i

agreements were observed among these methods for the large-scale rock discontinuities with $R^2 = 0.8844$ and 0.8471 , verifying the robustness of the proposed method.

Influence of rock joint roughness level on the appropriate sampling interval

Roughness coefficients (Z_2 and SD_i) were calculated for thirteen small-scale rock joint specimens under different sampling intervals in the laboratory. Similar trends were observed from the plots of sampling interval vs. roughness coefficients, and the roughness coefficients decreased as the sampling interval increased (Fig. 9). Afterwards, power functions were adopted to fit the data, and appropriate interval sampling was determined by calculating the curvature of each point. Table 3 lists

the fitting parameters a and b of 13 rock joint specimens that were determined based on Eq. (7) for Z_2 and SD_i methods, respectively. In addition, the length of curvature k for each sampling interval was calculated according to Eq. (8), and the sampling interval that had a maximum length of curvature k_{max} was considered as the appropriate sampling interval (cyan points in Fig. 9).

Figure 10 a illustrates that negative correlations between JRC (calculated based on Z_2 and SD_i methods, respectively) and the appropriate sampling interval were observed, following the linear distribution functions. It can be seen that a smaller interval was required to estimate the roughness of a rock joint with a rougher surface, and vice versa. For an absolutely smooth rock joint in an extreme situation, the point cloud obtained in a large sampling interval still can accurately represent morphology features of the rock joint; while for a rough rock joint, a fine measurement with a smaller sampling interval is required to avoid ignoring any details. Their relationships created based on Z_2 and SD_i could be described as,

$$\begin{cases} SI_a = -0.0481 \times JRC + 0.8045 & r^2 = 0.8500 & (Z_2) \\ SI_a = -0.0955 \times JRC + 2.5228 & r^2 = 0.9327 & (SD_i) \end{cases} \quad (10)$$

Furthermore, the JRC values calculated using Z_2 and SD_i methods in this study matched the roughness estimation obtained using Grasselli’s method. Both Table 4 and Fig. 10b provide more details about the comparison, and strong correlations among three methods were observed for the small-scale rock joint specimens through linear fitting analysis, with an R^2 of 0.9529 and 0.9047, respectively, proving the robustness of the proposed method again.

Discussions

Nevertheless, the linear fitting lines in Eq. (9) and Fig. 8a did not pass through the origin, causing unreasonable determination on the appropriate sampling interval when roughness estimation was performed for small size rock joints. For example, if the size of a rock joint was 60 mm, the appropriate sampling size would be specified as 7.2759 mm or 11.3865 mm based on Eq. (9), which were too large to collect the detailed information on the rock joint surface. The main cause of the intercept of Eq. (9) lied in there was an obvious size effect on JRC estimation for the 17 larger scale rock discontinuities (Fig. 11): JRC sharply decreased with sampling sizes ranging from 60 to 400 mm, followed by an increase on JRC when sampling size ranged from 500 to 800 mm, and then JRC slightly fluctuated between 10 and 14 with the increase of the sampling size. As a result, the JRC values of rock

Table 4 Summary of roughness estimation for 13 small-scale rock joint specimens calculated using three methods and appropriate sampling intervals

No	Size (mm)	JRC		C		θ_{max}^*		$\theta_{max}^*/(C + 1)$	
		Z_2	SD_i	Z_2	SD_i	Z_2	SD_i	Z_2	SD_i
JS-1	60	9.50	11.16	7841.6586	19.2863	81638.1924	197.7743	10.4095	9.7491
JS-2	60	0.08	3.61	15532.9826	14519.7024	60270.0839	40207.43	3.8799	2.769
JS-3	60	4.51	4.11	13020.267	4754.3905	60424.2327	17357.2968	4.6404	3.65
JS-4	60	14.55	13.69	3953.2429	2949.9881	51084.8283	35726.7726	12.919	12.1067
JS-5	60	0.75	2.34	11843.1969	11124.2109	42307.5765	29244.065	3.572	2.6286
JS-6	60	4.73	5.98	8112.3711	5935.3748	50692.3167	30252.8211	6.248	5.0962
JS-7	60	15.55	16.27	5037.9638	4781.3955	71536.7187	61291.6429	14.1967	12.8161
JS-8	60	6.40	7.93	9437.891	8.1009	71297.1572	56.7623	7.5536	6.237
JS-9	60	2.38	4.69	10918.5896	5.0568	61361.6993	27.7774	5.6194	4.5862
JS-10	60	8.75	11.17	8222.0502	2.6987	71325.6214	27.4414	8.6739	7.4192
JS-11	60	16.38	17.66	5.9483	4.0852	89.4254	53.2952	12.8701	10.4805
JS-12	60	12.41	12.73	5641.1474	43.0059	61250.5421	417.0368	10.8559	9.4768
JS-13	60	11.16	10.13	6997.6922	4822.6446	66280.3255	35542.7218	9.4704	7.3684

discontinuities varied from each other. Theoretically, to better understand the effect of sampling size on the appropriate sampling intervals, the roughness for all size rock joints should keep constant. However, it is impossible that natural joints with different scales have the same roughness level. Therefore, some calculation errors were introduced during investigating the effect of sampling size on the appropriate sampling interval mentioned in the “Influence of rock joint size on the appropriate sampling interval” section, due to the roughness difference.

Alternatively, to produce point clouds of rock joints with different sizes but without changing on roughness, the original point cloud of a small size joint specimen was proportionally resized in XYZ coordinates. In this

manner, eighteen artificial point clouds of joint specimens with different sizes (from 60 to 2000 mm) were generated. Meanwhile, 75 sampling intervals were set for each new joint, and the maximum and minimum interval was set as 37.5% and 0.5% of the side length, respectively. Then, roughness coefficients (Z_2 and SD_i) were computed based on Eqs. (1), (3), and (4). Figure 12 shows the variance of roughness coefficients with the sampling interval for 18 artificial point clouds. Similar changes on curves of sampling interval vs. roughness coefficient were observed. Also, a power function fitting analysis and curvature calculations were performed to identify appropriate sampling intervals from these curves. Two linear fitting lines with an intercept closing to 0 were obtained to describe the relationship between the sampling size and appropriate sampling interval (Fig. 13), which can be written as Eq. (11). Both formulas suggested that a larger sampling interval was required for a larger size rock joint so that the key geometrical information was not ignored and more accurate estimation was also achieved at the same time.

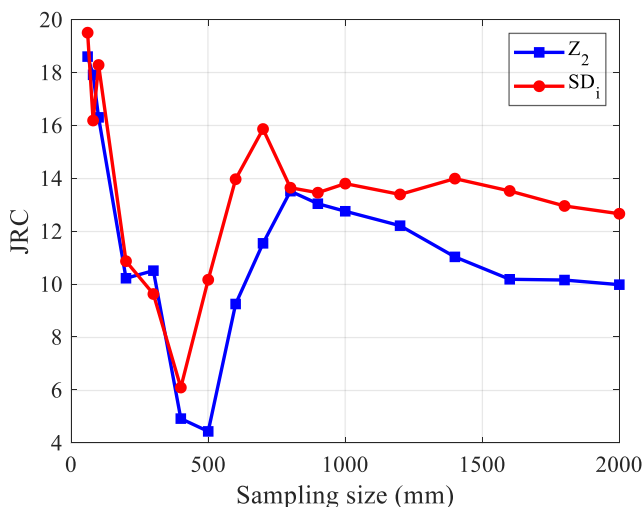


Fig. 11 Variance of JRC with the sampling size ranging from 60 to 2000 mm

$$\begin{cases} SI_a = 0.0150 \times SS + 0.3832 & 60mm \leq SS \leq 2000mm \quad r^2 = 0.9908 (Z_2) \\ SI_a = 0.0298 \times SS + 0.2057 & 60mm \leq SS \leq 2000mm \quad r^2 = 0.9846 (SD_i) \end{cases} \quad (11)$$

Several empirical equations—Eqs. (9), (10), and (11)—were proposed to estimate the appropriate sampling interval according to the sampling size and roughness level of rock joints. During performing roughness estimation of a given rock joint in practical engineering, the size of the interested rock joint is easy to be measured by using

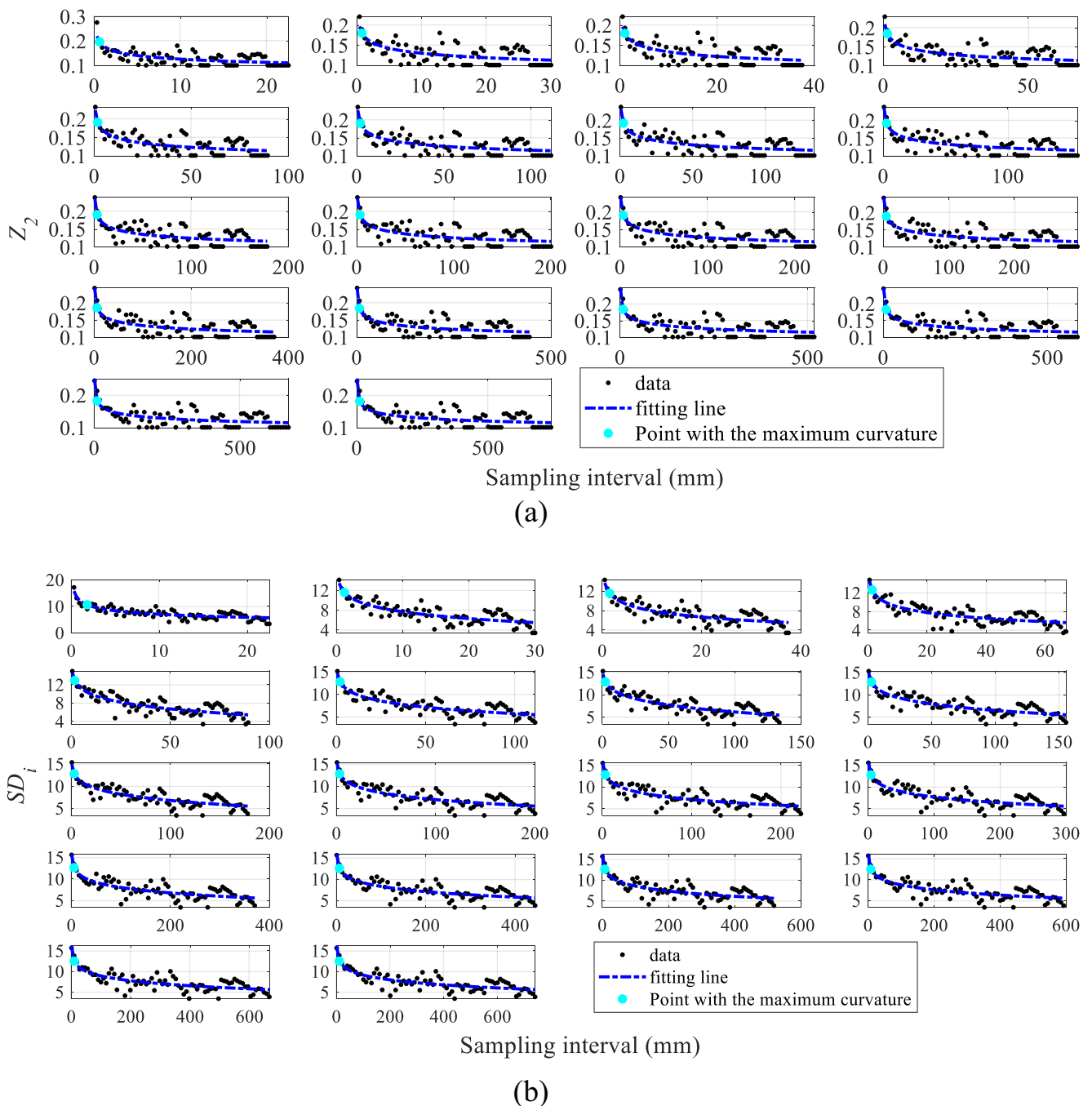


Fig. 12 Curves of sampling interval vs. sampling size for eighteen artificial rock joints (60–2000 mm): **a** Z_2 and **b** SD_i

common devices, such as a ruler and a laser meter, while the JRC of the rock joint is unknown, which is difficult to be calculated directly in the field. However, a general subjective understanding of the roughness level could be achieved through visual inspection, for example, ten standard profiles (Barton and Choubey 1977). Therefore, for a particular rock joint, an appropriate sampling interval is suggested to be determined mainly based on the sampling size. Because Eq. (11) has almost no intercept, to facilitate the application of the findings presented in this study

in a simple way, the appropriate sampling interval is suggested to be set as $0.015 \times \text{sampling size}$ (a small value) for a rock joint with a high-level roughness, due to the negative correlation between the roughness level and appropriate sampling interval (Eq. 10). For a low-level roughness rock joint, $0.03 \times \text{sampling size}$ (a large value) is recommended to be considered as the appropriate sampling interval. A flow chart was provided for a quick determination of the appropriate sampling interval in Fig. 14, and the main procedures are as follows:

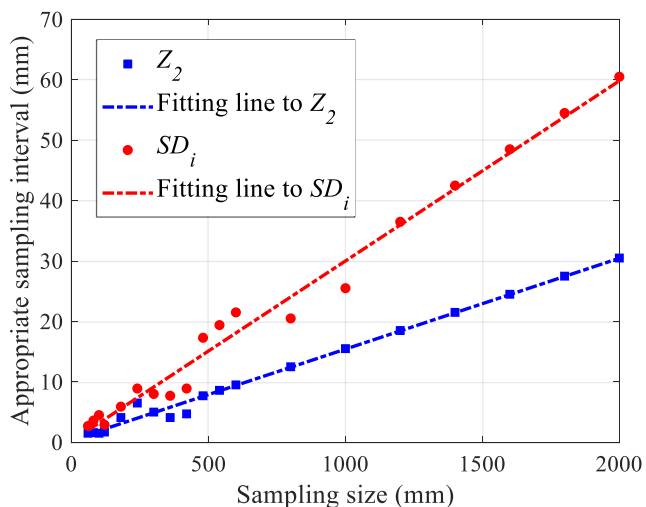


Fig. 13 The relationship between sampling size and appropriate sampling interval for artificial point clouds of joints

- (1) Preliminary study on the roughness level of a given rock joint, which was coarsely determined by comparing with ten standard profiles.
- (2) Measurement of the sampling size of the rock joint using common devices.
- (3) Determination of the appropriate sampling interval. For a rock joint with a high-level roughness, the appropriate sampling interval was specified as $0.015 \times \text{sampling size}$, whereas $0.030 \times \text{sampling size}$ for a rock joint with a low-level roughness.

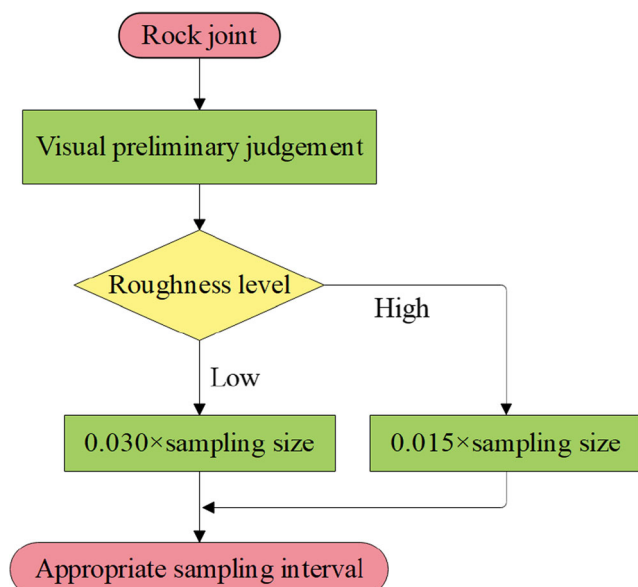


Fig. 14 Flow chart for quick determination of the appropriate sampling interval in practice

Conclusions

The sampling interval is an important parameter for roughness estimation of rock joint using laser scanning technique. To describe rock joint roughness accurately and effectively, it is necessary to choose an appropriate sampling interval to collect point clouds and perform roughness investigation. Based on above-mentioned analyses, the following conclusions of this study were drawn:

- (1) The effect of the sampling size on the selection of the appropriate sampling interval was investigated based on 17 rock discontinuities with different sampling size ranging from 60×60 to 2000×2000 mm in the field survey. Fitting analysis showed that there was a positive correlation between the sampling size and the appropriate sampling interval. Furthermore, a similar trend was observed for 18 artificial point clouds of joint specimens with the same roughness level but different sampling sizes.
- (2) Based on the point clouds collected by a portable laser scanner in the laboratory, 13 small-scale rock joint specimens with different roughness levels were used to assess the effect of roughness level on the selection of the appropriate sampling interval. The results demonstrated that the appropriate sampling interval decreased with the increase of the roughness level of rock joints.
- (3) A method was developed to detect the appropriate sampling interval from curves of the roughness coefficient vs. sampling interval that obeyed the power distribution. The inflection point with the maximum curvature on the curves was considered as the appropriate sampling interval. The roughness coefficients were more sensitive to the sampling intervals less than the inflection point. Under the condition of the appropriate sampling interval, the roughness estimation obtained using Z_2 and SD_i methods corresponded to the results of a 3D method.
- (4) To facilitate practical engineering applications, a simplified approach was proposed to determine the appropriate sampling interval: for a rock joint with a high-level roughness, it was suggested to specify the appropriate sampling interval as $0.015 \times \text{sampling size}$, while $0.03 \times \text{sampling size}$ was recommended to be considered as the appropriate sampling interval for a low-level roughness rock joint.

Acknowledgements Prof. Liangqing Wang and Dr. Changshuo Wang are acknowledged for their help in laboratory data collection. Special appreciation goes to the editor and two anonymous reviewers of this manuscript for their time and valuable comments.

Author contribution Conceptualization, Yunfeng Ge; methodology, Yunfeng Ge, Zishan Lin, and Binbin Zhao; formal analysis and investigation, Yunfeng Ge and Zishan Lin; writing (original draft preparation),

Yunfeng Ge and Zishan Lin; writing (review and editing), Yunfeng Ge and Zishan Lin; funding acquisition, Huiming Tang; resources, Yunfeng Ge and Huiming Tang; supervision, Yunfeng Ge and Huiming Tang.

Funding This study was funded by the National Key R&D Program of China (No. 2017YFC1501303 and 2018YFC1507200) organized by the Ministry of Science and Technology of China and the general program (No. 42077264) organized by the National Natural Science Foundation of China.

Data availability The data and materials that support the findings of this study are available from the first and corresponding author, Yunfeng Ge and Huiming Tang, upon reasonable request.

Code availability Codes that support the findings of this study are available from the first and corresponding author, Yunfeng Ge and Huiming Tang, upon reasonable request.

Declarations

Conflict of interest The authors declare no competing interests.

References

- Alameda-Hernández P, Jiménez-Perálvarez J, Palenzuela JA, El Hamdouni R, Irigaray C, Cabrerizo MA, Chacón J (2014) Improvement of the JRC calculation using different parameters obtained through a new survey method applied to rock discontinuities. *Rock Mech Rock Eng* 47(6):2047–2060. <https://doi.org/10.1007/s00603-013-0532-2>
- Bae DS, Kim KS, Koh YK, Kim JY (2011) Characterization of joint roughness in granite by applying the scan circle technique to images from a borehole televiewer. *Rock Mech Rock Eng* 44(4):497–504. <https://doi.org/10.1007/s00603-011-0134-9>
- Barton N (1973) Review of a new shear-strength criterion for rock joints. *Eng Geol* 7(4):287–332. [https://doi.org/10.1016/0013-7952\(73\)90013-6](https://doi.org/10.1016/0013-7952(73)90013-6)
- Barton N, Choubey V (1977) The shear strength of rock joints in theory and practice. *Rock Mech Rock Eng* 10(1-2):1–54. <https://doi.org/10.1007/BF01261801>
- Belem T, Souley M, Homand F (2007) Modeling surface roughness degradation of rock joint wall during monotonic and cyclic shearing. *Acta Geotech* 2(4):227–248. <https://doi.org/10.1007/s11440-007-0039-7>
- Fardin N, Stephansson O, Jing L (2001) The scale dependence of rock joint surface roughness. *Int J Rock Mech Min Sci* 38(5):659–669. [https://doi.org/10.1016/S1365-1609\(01\)00028-4](https://doi.org/10.1016/S1365-1609(01)00028-4)
- Feng Q, Fardin N, Jing L, Stephansson O (2003) A new method for in-situ non-contact roughness measurement of large rock fracture surfaces. *Rock Mech Rock Eng* 36(1):3–25. <https://doi.org/10.1007/s00603-002-0033-1>
- Ge YF, Tang HM, Wang LQ, Xiong CR (2013) Error analysis of sampling spacing on roughness of rock joint based on three dimensional laser scanning testing. In: 47th US Rock Mechanics/Geomechanics Symposium. American Rock Mechanics Association, San Francisco, pp 2226–2237
- Ge YF, Kulatilake PHSW, Tang HM, Xiong CR (2014) Investigation of natural rock joint roughness. *Comput Geotech* 55(1):290–305. <https://doi.org/10.1016/j.compgeo.2013.09.015>
- Ge YF, Tang HM, Eldin MAME, Chen PY, Wang LQ, Wang JG (2015) A description for rock joint roughness based on terrestrial laser scanner and image analysis. *Sci Rep* 5:16999. <https://doi.org/10.1038/srep16999>
- Ge YF, Tang HM, Eldin MAME, Wang LQ, Wu Q, Xiong CR (2017) Evolution process of natural rock joint roughness during direct shear tests. *Int J Geomech* 17(5):E4016013
- Ge YF, Lin ZS, Tang HM, Zhao BB, Chen HZ, Xie ZG, Du B (2020) Investigation of the effects of nonstationary features on rock joint roughness using the laser scanning technique. *Bull Eng Geol Environ* 79:1–12. <https://doi.org/10.1007/s10064-020-01754-6>
- Grasselli G (2001) Shear strength of rock joints based on quantified surface description (Thesis). EPFL, Lausanne.
- Grasselli G, Egger P (2003) Constitutive law for the shear strength of rock joints based on three-dimensional surface parameters. *Int J Rock Mech Min Sci* 40(1):25–40. [https://doi.org/10.1016/S1365-1609\(02\)00101-6](https://doi.org/10.1016/S1365-1609(02)00101-6)
- Han B, Zhang GB, Lan HX, Yan CG, Xu JB, Xu W (2020) Geometrical heterogeneity of the joint roughness coefficient revealed by 3D laser scanning. *Eng Geol* 265:105415. <https://doi.org/10.1016/j.enggeo.2019.105415>
- Hong ES, Lee JS, Lee IM (2008) Underestimation of roughness in rough rock joints. *Int J Numer Anal Methods Geomech* 32(11):1385–1403. <https://doi.org/10.1002/nag.678>
- International Society for Rock Mechanics (ISRM) (1978) Suggested methods for the quantitative description of discontinuities in rock masses. *Int J Rock Mech Min Sci Geomech Abstr* 15:319–368
- Jang HS, Kang SS, Jang BA (2014) Determination of joint roughness coefficients using roughness parameters. *Rock Mech Rock Eng* 47(6):2061–2073
- Jiang YJ, Li B, Tanabashi Y (2006) Estimating the relation between surface roughness and mechanical properties of rock joints. *Int J Rock Mech Min Sci* 43(6):837–846. <https://doi.org/10.1016/j.ijrmms.2005.11.013>
- Jiang Q, Yang B, Yan F, Liu C, Shi YG, Li LF (2020) New method for characterizing the shear damage of natural rock joint based on 3D engraving and 3D scanning. *Int J Geomech* 20(2):06019022. [https://doi.org/10.1061/\(ASCE\)GM.1943-5622.0001575](https://doi.org/10.1061/(ASCE)GM.1943-5622.0001575)
- Kim DH, Gratchev I, Balasubramaniam A (2013) Determination of joint roughness coefficient (JRC) for slope stability analysis: a case study from the Gold Coast area, Australia. *Landslides* 10(5):657–664. <https://doi.org/10.1007/s10346-013-0410-8>
- Kulatilake PHSW, Shou G, Huang TH, Morgan RM (1995) New peak shear strength criteria for anisotropic rock joints. *Int J Rock Mech Min Sci Geomech Abstr* 32(7):673–697. [https://doi.org/10.1016/0148-9062\(95\)00022-9](https://doi.org/10.1016/0148-9062(95)00022-9)
- Kulatilake PHSW, Balasingam P, Park J, Morgan RM (2006) Natural rock joint roughness quantification through fractal techniques. *Geotech Geol Eng* 24(5):1181–1202. <https://doi.org/10.1007/s10706-005-1219-6>
- Kumar R, Verma AK (2016) Anisotropic shear behavior of rock joint replicas. *Int J Rock Mech Min Sci* 90:62–73. <https://doi.org/10.1016/j.ijrmms.2016.10.005>
- Kumar R, Verma AK (2020) Corrections applied to direct shear results and development of modified Barton's shear strength criterion for rock joints. *Arab J Geosci* 13:1019. <https://doi.org/10.1007/s12517-020-06030-1>
- Kusumi H, Teraoka K, Nishida K (1997) Study on new formulation of shear strength for irregular rock joints. *Int J Rock Mech Min Sci* 34(3-4):1680–2147483647. [https://doi.org/10.1016/s1365-1609\(97\)00029-4](https://doi.org/10.1016/s1365-1609(97)00029-4)
- Lee YH, Carr JR, Barr DJ, Haas CJ (1990) The fractal dimension as a measure of the roughness of rock discontinuity profiles. *Int J Rock Mech Min Sci Geomech Abstr* 27(6):453–464. [https://doi.org/10.1016/0148-9062\(90\)90998-h](https://doi.org/10.1016/0148-9062(90)90998-h)
- Lee SD, Lee CI, Park Y (1997) Characterization of joint profiles and their roughness parameters. *Int J Rock Mech Min Sci* 34(3-4):1740–17400000. [https://doi.org/10.1016/s1365-1609\(97\)00083-x](https://doi.org/10.1016/s1365-1609(97)00083-x)

- Li Y, Wu W, Li B (2018) An analytical model for two-order asperity degradation of rock joints under constant normal stiffness conditions. *Rock Mech Rock Eng* 51(5):1431–1445. <https://doi.org/10.1007/s00603-018-1405-5>
- Liu R, Li B, Jiang Y (2016) Critical hydraulic gradient for nonlinear flow through rock fracture networks: the roles of aperture, surface roughness, and number of intersections. *Adv Water Resour* 88:53–65
- Liu Q, Tian Y, Liu D, Jiang Y (2017) Updates to JRC-JCS model for estimating the peak shear strength of rock joints based on quantified surface description. *Eng Geol* 228:282–300. <https://doi.org/10.1016/j.enggeo.2017.08.020>
- Maerz NH, Franklin JA, Bennett CP (1990) Joint roughness measurement using shadow profilometry. *Int J Rock Mech Min Sci Geomech Abstr* 27(5):329–343. [https://doi.org/10.1016/0148-9062\(90\)92708-M](https://doi.org/10.1016/0148-9062(90)92708-M)
- Mah J, Samson C, McKinnon SD, Thibodeau D (2013) 3D laser imaging for surface roughness analysis. *Int J Rock Mech Min Sci* 58:111–117. <https://doi.org/10.1016/j.ijmms.2012.08.001>
- Patton FD (1966) Multiple modes of shear failure in rock. In: *Proceedings of the 1st congress of the international society of rock mechanics*, Lisbon, Portugal, September/October 1966, 1: 509–513.
- Reeves MJ (1985) Rock surface roughness and frictional strength. *Int J Rock Mech Min Sci Geomech Abstr* 22(6):429–442. [https://doi.org/10.1016/0148-9062\(85\)90007-5](https://doi.org/10.1016/0148-9062(85)90007-5)
- Stigsson M, Ivars DM (2019) A novel conceptual approach to objectively determine JRC using fractal dimension and asperity distribution of mapped fracture traces. *Rock Mech Rock Eng* 52(4):1041–1054. <https://doi.org/10.1007/s00603-018-1651-6>
- Sun SY, Li YC, Tang CA, Li B (2019) Dual fractal features of the surface roughness of natural rock joints. *Chin J Rock Mech Eng* 38(12): 2502–2511
- Tang HM, Ge YF, Wang LQ, Yuan Y, Huang L, Sun MJ (2012) Study on estimation method of rock mass discontinuity shear strength based on three-dimensional laser scanning and image technique. *J Earth Sci* 23(6):908–913 CNKI:SUN:ZDDY.0.2012-06-014
- Tang HM, Wasowski J, Juang CH (2019) Geohazards in the three Gorges Reservoir Area, China—lessons learned from decades of research. *Eng Geol* 261:105267
- Tatone BSA, Grasselli G (2010) A new 2D discontinuity roughness parameter and its correlation with JRC. *Int J Rock Mech Min Sci* 47(8):1391–1400. <https://doi.org/10.1016/j.ijmms.2010.06.006>
- Tatone BSA, Grasselli G (2013) An investigation of discontinuity roughness scale dependency using high-resolution surface measurements. *Rock Mech Rock Eng* 46(4):657–681. <https://doi.org/10.1007/s00603-012-0294-2>
- Tse R, Cruden DM (1979) Estimating joint roughness coefficients. *Int J Rock Mech Min Sci Geomech Abstr* 16(5):303–307. [https://doi.org/10.1016/0148-9062\(79\)90241-9](https://doi.org/10.1016/0148-9062(79)90241-9)
- Ünlüsoy D, Süzen ML (2020) A new method for automated estimation of joint roughness coefficient for 2D surface profiles using power spectral density. *Int J Rock Mech Min Sci* 125:104156
- Wang LQ, Wang CS, Khoshnevisan S, Ge YF, Sun ZH (2017) Determination of two-dimensional joint roughness coefficient using support vector regression and factor analysis. *Eng Geol* 231:238–251. <https://doi.org/10.1016/j.enggeo.2017.09.010>
- Wang M, Wan W, Zhao YL (2020) Determination of joint roughness coefficient of 2D rock joint profile based on fractal dimension by using of the gene expression programming. *Geotech Geol Eng* 38(1):861–871. <https://doi.org/10.1007/s10706-019-01070-1>
- Xie HP, Wang JA, Xie WH (1997) Fractal effects of surface roughness on the mechanical behavior of rock joints. *Chaos, Solitons Fractals* 8(2):221–252. [https://doi.org/10.1016/s0960-0779\(96\)00050-1](https://doi.org/10.1016/s0960-0779(96)00050-1)
- Yang ZY, Lo SC, Di CC (2001) Reassessing the joint roughness coefficient (JRC) estimation using Z2. *Rock Mech Rock Eng* 34(3):243–251
- Yang ZY, Taghichian A, Li WC (2010) Effect of asperity order on the shear response of three-dimensional joints by focusing on damage area. *Int J Rock Mech Min Sci* 47(6):1012–1026
- Yong R, Ye J, Li B, Du SG (2018) Determining the maximum sampling interval in rock joint roughness measurements using Fourier series. *Int J Rock Mech Min Sci* 101:78–88. <https://doi.org/10.1016/j.ijmms.2017.11.008>
- Yu XB, Vayssade B (1991) Joint profiles and their roughness parameters. *Int J Rock Mech Min Sci Geomech Abstr* 28(4):333–336